

# Ultrasound Localization of Microbubbles for Active Microrheology of Viscoelastic Media

*Anne-Lise DUROY*<sup>1</sup>, *Antoine PENNERON*<sup>1</sup>, *Thomas BRUNET*<sup>1</sup>, and *Diego BARESCH*<sup>1</sup>

<sup>1</sup>*Univ. Bordeaux, CNRS, Bordeaux INP, I2M, UMR 5295, F-33400, Talence, France*  
*anne-lise.duroy@u-bordeaux.fr, diego.baresch@u-bordeaux.fr*

**Abstract:** Investigating the mechanical properties of biological media over several scales is important for our fundamental understanding of complex biological processes. In this paper, an active microrheology approach for viscoelastic media is proposed, which relies on the use of acoustical tweezers to force individual microbubbles and the ultrasound localization of its induced displacement. Our study shows that a good localization accuracy is achieved and can resolve displacements that are typically observed under acoustic forcing experiments.

**Keywords:** Microrheology, Ultrasound localization, Acoustical tweezers, Microbubbles, Viscoelasticity

## Introduction

From tissues to single cells, investigating the mechanical properties of biological media is essential to study biological processes, and for diagnostic and treatment purposes. It is now known that developing organisms are sensitive to their mechanical environment, and that there is a reciprocal feedback between mechanosensing mechanisms at the cellular scale and the macroscopic properties of tissue [1]. Thus, methods to probe the biomechanical properties of complex systems over several length and time scales are required to provide a finer understanding of the fundamental phenomena involved in the emerging field of mechanobiology.

Several experimental techniques have been developed to actively probe the rheological properties of complex biological systems by manipulating small probe particles *in situ*, and can operate from the sub-cellular to the multi-cellular tissue scales [2, 3, 4, 5]. For instance, optical tweezers are precise, efficient and versatile tools for manipulation at the sub-cellular scale, but do not easily penetrate into thick, generally opaque-to-light media, and generate weak forces (10-100 pN) despite the high light intensities required, limiting their use at the multi-cellular scale. Magnetic tweezers can generate larger forces (1-100 nN), but they are applied along one direction fixed by the orientation of the magnetic field, making them not well adapted to characterize anisotropic and heterogeneous media. Very recently, acoustic approaches have emerged and highlight the suitability of using the high magnitude radiation forces (1-1000 nN) to probe the rheology of a variety of bulky soft biological materials [6, 7]. In this context, further removing the need for optical imaging methods to track the displacement of the probe particles could open interesting perspectives

for the microrheological characterization of a range of currently inaccessible biological systems at the cellular and multi-cellular levels.

In this paper, we propose a proof-of-concept for a method based on the ultrasonic localization of microbubbles displaced by the radiation force generated in acoustical tweezers [7]. Originally developed for vascular imaging, Ultrasound Localization Microscopy (ULM) can provide super-resolution images by tracking the displacement of a large number of microbubbles (MBs) over time using high frame rate ultrasound images [8]. Implementing an ultrasound localization method within the framework of active microrheology could be promising provided the following requirements are met: (i) minute displacements of a MB in response to an applied force are detected, (ii) this detection is obtained with a good spatio-temporal resolution, and (iii) the localization remains robust for MBs embedded in media of increasing complexity. Here, we consider the tracking of an individual MB embedded in a simple viscoelastic media and show that the precision of the localization combined with the good temporal resolution afforded by programmable ultrasonic platforms can allow to assess local rheological properties.

## Numerical Method

Several approaches are available to implement ULM methods [8, 9, 10]. Yet, they are all based on detecting and tracking of numerous MBs over time using their characteristic isolated signatures within ultrasound images. In the application proposed here, our focus is on the localization of a single MB whose displacement will be imposed by the local force generated by acoustical tweezers.

Because of their small size ( $R_0 \ll \lambda$ ), where  $\lambda$  is

the imaging wavelength, MBs can be considered as punctual scatterers whose a spherical wave propagating outwards, resulting in a characteristic wavefront (hyperbola) that can be distinguished in raw (or radio-frequency, RF) images [11]. The shape and position of this hyperbola can be described by the time-of-flight (Tof), or the time for the emitted signal to travel through the medium to the MB position  $(z, x)$  and back to a transducer element  $(z_e, x_e)$ . Assuming a constant speed of sound,  $c_0$ , and considering an incident plane wave illumination, the Tof equation reads:

$$\tau = \frac{z + \sqrt{(z_e - z)^2 + (x_e - x)^2}}{c_0}. \quad (1)$$

Thus, a MB can simply be localized within ultrasound images by timing on each element the arrival of the spherical wavefront in the RF image and fitting the experimental hyperbola to the Tof equation, with  $(z, x)$  as a couple of adjusting parameters. To obtain the images, numerical simulations are built using the *k-Wave*<sup>®</sup> open-source toolbox[12]. Space and time are discretized on a regular grid, and the acoustic field is computed at each node of the mesh. To simulate pulse-echo RF images, grid points in the transducer regions are both sources and sensors. More specifically, grid points corresponding to the active elements are modeled as time varying pressure sources, while those within the kerf are left empty. At reception, the signals are averaged over the grid points describing each element, and down-sampled to match a realistic sampling frequency of common ultrasonic imaging platforms. The medium can either be considered homogeneous, with mechanical properties corresponding to water, or contained inhomogeneities by introducing spatial fluctuations of the density and speed of sound values using a normal distribution with standard deviation  $\sigma$  around the properties of water.

Adopting a similar workflow to that described in Ref.[13], the RF images are computed as follows:

1. An incident plane wave is emitted within the medium without considering the MB existence. The pressure field generated by medium inhomogeneities ( $P_m$ ) is recorded at the transducer positions. Simultaneously, the pressure is computed at the MB positions to estimate the pressure ( $P_{ac}$ ) experienced by the MB.
2. The MB response to  $P_{ac}$  is computed using the nonlinear Marmottant model [14], and the pressure field scattered by the MB ( $P_s$ ) is determined on the bubble surface and re-injected as a punctual pressure source.
3. The scattered field  $P_s$  is finally propagated in the direction of the receivers, and added to the

back-scattered field  $P_m$ , to form the final RF image.

Consecutive RF images for a moving MB are built by repeating step 2 – 3 for the different positions of the MB, and for the different imaging probe parameters presented below.

To obtain the hyperbola within RF images, a Hilbert transform is applied to the received signals to extract the pulse envelope. Then, a rectangular region of interest (ROI) containing the MB echo is defined through the normalized cross-correlation between the envelope and that of the emitted signal. Indeed, it is expected that the MB back-scattered pulse will be highly correlated with the emitted signal. The correlation threshold defining the ROI is chosen as a trade-off between a minimal size of the ROI, and a minimal Signal-to-noise ratio (SNR) of the received signals. Finally, we determine the experimental hyperbola by timing the arrival of the maximum of the envelop. Finally, a fit to Eq. (1) using a non-linear regression algorithm provides an estimation of the MB position  $(z, x)$ .

## Results and discussion

Let us first consider a perfectly homogeneous medium imaged with a 5MHz imaging probe (pitch: 600  $\mu\text{m}$ , sampling frequency:  $f_s = 25$  MHz), and containing a single MB. The MB is displaced along a two-dimensional path defined by 9 successive positions (Fig. 1-a). The path is located beneath the central element of the imaging probe at a depth of 10 mm. We are interested in the errors,  $(\delta_u, \delta_v)$ , inherent to the localization method for the detection of the MB displacement vector  $(u, v)$ , where  $u = z_{i+1} - z_i$  and  $v = x_{i+1} - x_i$  are obtained at MB positions  $i$  and  $i+1$  (Fig. 1-b,c). It is seen that the localized displacement is very close to the ground truth in both directions. The estimated errors are approximately  $\delta_u \sim \frac{\lambda}{60}$  and  $\delta_v \sim \frac{\lambda}{15}$  in the axial and lateral directions respectively. The better performance in the vertical direction can be ascribed to the good temporal sampling ( $1/f_s$ ) that allows for a precise timing of the MB back-scattered pulse arrival, whereas the accuracy in the lateral direction is limited by the aperture and the number of transducer elements [11]. Since distant imaging elements can rapidly suffer from a low SNR, a restricted ROI has to be defined as discussed above.

Next we explore the influence of three different parameters on the displacement error estimation: the strength of the medium inhomogeneities (image speckle) in Figure 2-a, the pitch of the imaging probe (aperture) in Figure 2-b, and the central frequency  $F_0$  in Figure 2-c. It can be observed that the displacement precision decreases in both directions with

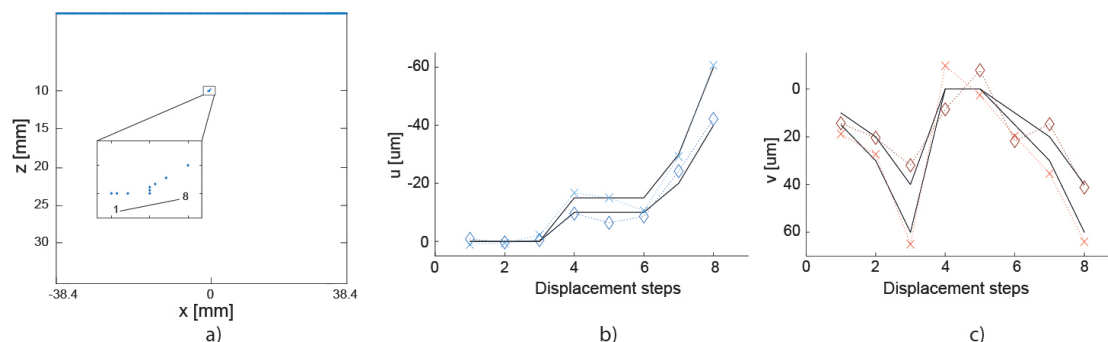


Fig. 1: (a) Scheme of a homogeneous medium imaged using a  $600 \mu\text{m}$  pitch transducer with a central frequency of  $5\text{MHz}$ , where each point represents the MB displacement steps. (b) Axial  $u$  and (c) lateral  $v$  displacement components. The black lines show the ground truth, and the color diamonds the results for different data sets obtained by changing the magnitude of the displacement steps in the initial path.

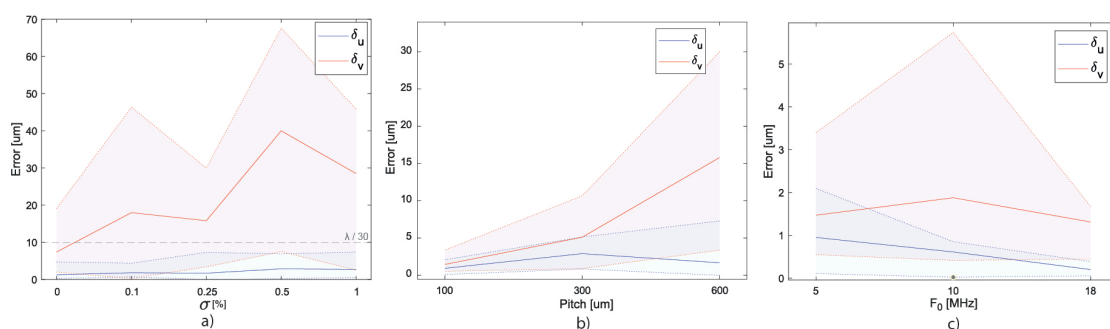


Fig. 2: Estimated axial  $\delta_u$  (blue) and lateral  $\delta_v$  (red) displacement errors as a function of: (a)  $\sigma$  (or speckle level in the image), (b) the pitch of the transducer and (c) the central frequency  $F_0$ . Solid lines show the median error, and the shaded regions the dispersion of the results.

increasing  $\sigma$ , with a prominent influence on  $\delta_v$ , because of the degraded SNR. However, the increase of  $\delta_u$  is very limited, suggesting that the proposed tracking approach will be robust in the axial direction for media of increasing complexity. Regarding the influence of the pitch of the 128-element probe, a net increase in the precision is observed in both directions when the pitch is decreased. This result confirms that the main contribution to the error arises from a degraded SNR on the lateral extremities of the probe. Therefore, it is better to reduce the physical aperture of the probe if the SNR is expected to be poor on the sides and populate this aperture with a maximum number of elements. This result is also suggested in Ref.[11]. Finally, the influence of the central imaging frequency shows that, whereas the error is low for  $F_0 = 5$  and  $18$  MHz, it surprisingly increases for  $F_0 = 10$  MHz. This result is possibly due to a decrease in the scattering cross-section of a single MB relatively close but away from the MB resonance, that will then increase again for a higher frequency. This result suggests that properly understanding the

physics of the bubble oscillations is important to set the parameter space for future experiments. It's also worth noting that the estimated MB displacement is always more accurate in the axial direction, and is therefore preferred hereafter.

To finish, a proof of concept for the tracking of a single MB in a typical active microrheology experiment performed in a viscoelastic medium having a shear modulus  $\mu = 1$  kPa, a viscosity  $\eta = 0.1$  Pa.s, and a mild level of inhomogeneities ( $\sigma = 0.25$  %) is shown in Figure 3. Using an external force of  $50 \mu\text{N}$  generated by acoustical tweezers [7], a MB (radius  $R_0 = 20 \mu\text{m}$ ) is displaced from its initial position during a  $10$  ms radiation force pulse in the axial direction of the imaging probe. The theoretical curve is computed using a rheological model [15] and used as the ground truth trajectory. Using a 128-element imaging probe of  $18$  MHz central frequency and a pitch of  $100 \mu\text{m}$ , we can see that the localization method presented here is able to capture very accurately the trajectory of the displaced MB. Therefore, in a situation where the medium's properties are unknown, the

accurate detection of the MB displacements could provide a micromechanical characterization of the medium using a rheological model.

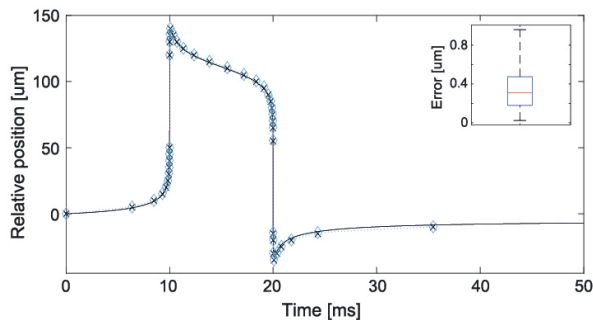


Fig. 3: Typical displacement of a single MB in an active rheology experiment. Solid line show the ground truth, the color diamonds the results, and the box-plot the estimated errors.

### Conclusion

In summary, a tracking method for active microrheology experiments with ultrasound was presented. A single MB is forced with acoustical tweezers and the induced displacement is tracked via the sub-wavelength ultrasound localization of the MB. Our results suggest that the good localization precision, especially in the axial direction, of a high frequency imaging probe is well-suited to track complex MB displacements in two-dimensions, showing a promising route for the local micro-mechanical characterization of a variety of complex media, including biological tissues.

### References

- [1] J. M. Barnes, L. Przybyla and V. M. Weaver, 'Tissue mechanics regulate brain development, homeostasis and disease,' *Journal of Cell Science*, vol. 130, no. 1, pp. 71–82, 2017.
- [2] K. Svoboda and S. M. Block, 'Biological applications of optical forces,' *Annual review of biophysics and biomolecular structure*, vol. 23, pp. 247–85, 1994.
- [3] P. Roca-cusachs, V. Conte and X. Trepac, 'Quantifying forces in cell biology,' *Nature Publishing Group*, 2017.
- [4] Y. L. Han et al., 'Cell swelling and softening and invasion in a and three-dimensional breast cancer model,' *Nature physics*, vol. 16, pp. 101–108, 2019.
- [5] G. Laloy-Borgna et al., 'Magnetic microelastography for evaluation of ultrasound-induced softening of pancreatic cancer spheroids,' *Physical Review Applied*, vol. 22, no. 2, p. 024 024, 2024.
- [6] G. Bergamaschi et al., 'Viscoelasticity of diverse biological samples quantified by Acoustic Force Microrheology (AFMR),' *Communications Biology*, vol. 7, no. 1, 2024.
- [7] A. Penneron, T. Brunet and D. Baresch, 'Active rheology of soft solids performed with acoustical tweezers,' *Applied Physic Lette*, vol. 126, p. 084 104, 2025.
- [8] O. Couture, V. Hingot, B. Heiles, P. Muleki-Seya and M. Tanter, 'Ultrasound localization microscopy and super-resolution: A state of the art,' *IEEE Transactions on Ultrasonics, Ferroelectrics, and Frequency Control*, vol. 65, no. 8, pp. 1304–1320, 2018.
- [9] K. Christensen-Jeffries et al., 'Super-resolution ultrasound imaging,' *Ultrasound in Medicine & Biology*, vol. 46, no. 4, pp. 865–891, 2020.
- [10] C. Hahne, G. Chabouh, A. Chavignon, O. Couture and R. Sznitman, 'Rf-uhl: Ultrasound and localization microscopy and learned from radio-frequency and wavefronts,' *IEEE Transactions on Medical Imaging*, 2023.
- [11] Y. Desailly, J. Pierre, O. Couture and M. Tanter, 'Resolution limits of ultrafast ultrasound localization microscopy,' *Physics in medicine & biology*, vol. 60, pp. 8723–8740, 2015.
- [12] B. Treeby, J. Jaros, A. Rendell and B. Cox, 'Modeling nonlinear ultrasound propagation in heterogeneous media with power law absorption using a k-space pseudospectral method,' *Journal of the Acoustical Society of America*, vol. 131, no. 6, pp. 4324–4336, 2012.
- [13] J. Brown et al., 'Investigation of microbubble detection methods for super-resolution imaging of microvasculature,' *IEEE Transactions on Ultrasonics, Ferroelectrics, and Frequency Control*, vol. 66, no. 4, pp. 676–691, 2019.
- [14] P. Marmottant et al., 'A model for large amplitude oscillations of coated bubbles and accounting for buckling and rupture,' *Journal of the Acoustical society of america*, vol. 118, pp. 3499–3505, 2005.
- [15] Y. a. Ilinskii, G. D. Meegan, E. a. Zabolotskaya and S. Y. Emelianov, 'Gas bubble and solid sphere motion in elastic media in response to acoustic radiation force,' *The Journal of the Acoustical Society of America*, vol. 117, no. 4, p. 2338, 2005.